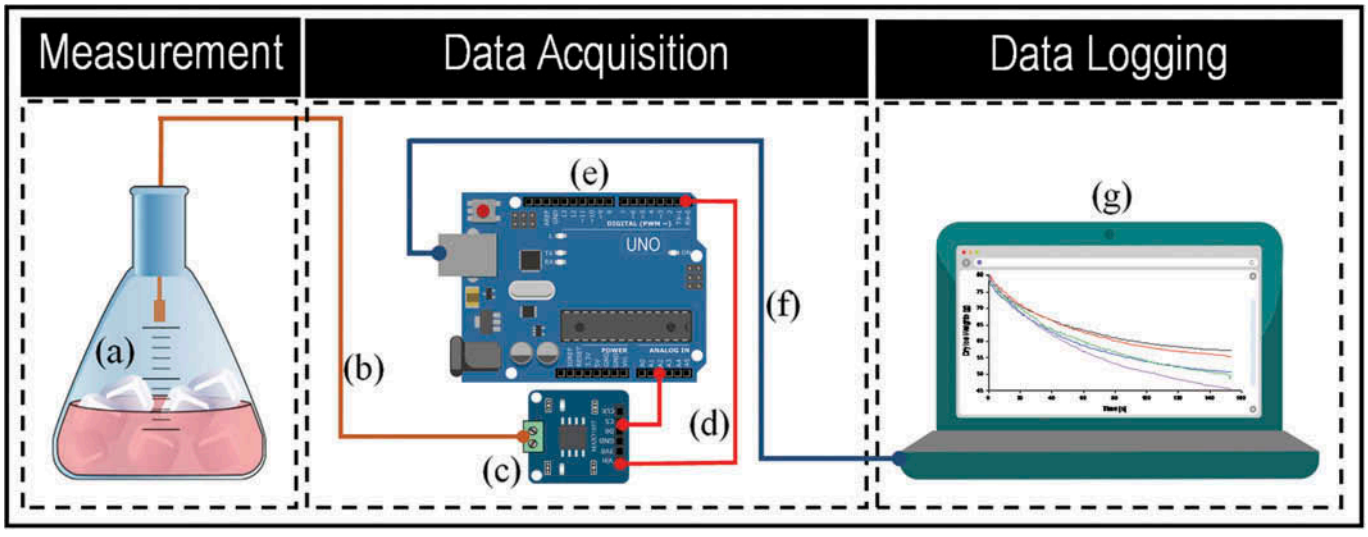

MECHANICAL ENGINEERING | RESEARCH ARTICLE

Optimization of CO_2 production rate for fire-fighting robot applications using response surface methodology

M. T. Ajala, Md R. Khan, A. A. Shafie, M. J. E. Salami, M. I. Mohamad Nor and M. O. Oladokun

Cogent Engineering (2018), 5: 1555744

Ajala et al., *Cogent Engineering* (2018), 5: 1555744
https://doi.org/10.1080/23311916.2018.1555744

cogent engineering

MECHANICAL ENGINEERING | RESEARCH ARTICLE

Optimization of CO_2 production rate for firefighting robot applications using response surface methodology

M. T. Ajala[1,2*], Md R. Khan[1], A. A. Shafie[1], M. J. E. Salami[3], M. I. Mohamad Nor[4] and M. O. Oladokun[5]

Received: 03 September 2018
Accepted: 30 November 2018
First Published: 05 December 2018

*Corresponding author: M. T. Ajala, Department of Mechatronics Engineering, International Islamic University Malaysia, Gombak, Kuala Lumpur, Malaysia; Department of Industrial Maintenance Engineering, Yaba College of Technology, Yaba, Lagos State, Nigeria
E-mail: mosud.ajala@yahoo.com; mosud.ajala@yabatech.edu.ng

Reviewing editor:
Wei Meng, Wuhan University of Technology, China

Additional information is available at the end of the article

Abstract: A carbon dioxide gas-powered pneumatic actuation has been proposed as a suitable power source for an autonomous firefighting robot (CAFFR), which is designed to operate in an indoor fire environment in our earlier study. Considering the consumption rate of the pneumatic motor, the gas-powered actuation that is based on the theory of phase change material requires optimal determination of not only the sublimation rate of carbon dioxide but also the sizing of dry ice granules. Previous studies that have used the same theory are limited to generating a high volume of carbon dioxide without reference to neither the production rate of the gas nor the size of the granules of the dry ice. However, such consideration remains a design requirement for efficient driving of a carbon dioxide-powered firefighting robot. This paper investigates the effects of influencing design parameters on the sublimation rate of dry ice for powering a pneumatic motor. The optimal settings of these parameters that maximize the sublimation rate at the minimal time and dry ice mass are presented. In the experimental design and analysis, we employed full-factorial design and response surface methodology to fit an acceptable model for the relationship between the design factors and the response variables. Predictive models of the sublimation rate were examined via

M. T. Ajala

ABOUT THE AUTHOR

The central focus of our research group is to develop autonomous systems and robots for different real-life applications like biomimetic robots, terrain mapping robots, disaster handling robots, etc. The proposed project falls under the disaster handling category. An autonomous firefighting robot (FFR) that can replace firefighters in fire hot spots to perform firefighting tasks is proposed here. Existing firefighting robots use prime movers that are electrically powered and vulnerable to a high-temperature environment. We introduced a carbon dioxide gas powered actuator for the propulsion of the FFR in the fire scene. The FFR will self-generate the required power for the actuator from dry ice using the theory of Phase Change of Material. The investigation in the present article provides the groundwork for the optimization of the dry ice to be used as the power source and also forms the basis for the completion of the prototype development.

PUBLIC INTEREST STATEMENT

Electric motor powered robots cannot operate close to fire spots because of the risk of insulation breakdown of the engines. A carbon dioxide (CO_2) gas-powered pneumatic actuator that can self-generate CO_2 *in situ* from dry ice has been proposed to replace the electrical motors and make actuator operable in indoor firefighting application.

To generate the CO_2 effectively from dry ice for the pneumatic power task, the effects of the influencing factors such as the mass of dry ice and the temperature of water—used as to speed up the production rate of carbon dioxide—on the sublimation rate of carbon dioxide from dry ice is examined in the current article.

Although the pneumatic motor, in this study, will be used to propel a firefighting robot in the high thermal indoor fire; the same approach is applicable for converting solid CO_2 into gas form for other applications.

ANOVA, and the suitability of the linear model is confirmed. Further, an optimal sublimation rate value of 0.1025 g/s is obtained at a temperature of 80°C, the mass of 16.1683 g, and sublimation time of 159.375 s.

Subjects: Power & Energy; Robotics & Cybernetics; Mechatronics

Keywords: air motor; dry ice; firefighting robot; Gas actuator; indoor fire; Phase Change Materials (PCM); pneumatic actuator; pneumatic motor; response surface methodology; sublimation rates

1. Introduction

Fire disasters around the world have continuously caused significant human casualties and collateral losses, and often, well-trained firefighters may succumb to injuries. The 68,085 firefighters' injuries that occurred in the line of duty during the year 2016 (Haynes & Molis, 2016) suggest that firefighting still presents great risks of personal injury to firefighters. Leveraging on the recent technological developments, robots are being used to lessen the injuries of firefighters and increase their work performance. As such, firefighting robot (FFR) are being developed for both indoor and outdoor applications with a broad objective of replacing and assisting the firefighters (Amano, 2002).

Research trends in the developments of FFR have shown that little attention has been paid to the design of the propulsion systems (AlHaza, Alsadoon, Alhusinan, Jarwali, & Alsaif, 2015), especially in extreme temperature. The mode of propulsion of the majority of the FFRs is by electrical power which has an unreliable performance in the extreme temperatures (Zhang, Kitagawa, & Tsukagoshi, 1999). Therefore, mobility and survival of FFR under high-temperature environment become a significant research area. As such Zhang et al. (1999) proposed a water-powered hydraulic propulsion system (WHPS) for the mobility of FFR in a severe temperature environment. The WHPS composed of a hydraulic motor as the actuator and water as the powering fluid instead of oil. The same mechanism was employed for a snake firefighting robot in a tunnel fire application by Liljeback, Stavdahl, and Beitnes (2006). However, while the latter has been designed for an outdoor application, the former lacks autonomous characteristic as required for current FFR.

To overcome the above challenges, a gas-actuated FFR is proposed in our earlier study (Ajala, Khan, Shafie, & Salami, 2016). The study conceived a novel carbon dioxide (CO_2) gas-powered autonomous firefighting robot (CAFFR). The said CAFFR is designed to be propelled by a pneumatic motor that is powered by *in situ* generated CO_2 gas from dry ice. Findings from the preliminary investigations revealed the possibility of generating low-pressure CO_2 gas as a power source for the gas-driven motor.

The CAFFR adopted the concept of phase change of materials (PCM) as its underlining theory. The theory was used to develop actuators (mainly linear actuators) that operate under the high thermal environment (Suzumori, Matsuoka, & Wakimoto, 2012; Matsuoka, & Suzumori, 2014; Matsuoka, Suzumori, & Kanda, 2016). These developments have been applied majorly in the area of material handling of equipment. Also, PCM was introduced in a robotic application with the development of a rubber bellow-based pneumatic actuator for the mobility of a pipe inspection robot (Ono & Kato, 2010).

Similarly, PCM has been used to develop pressure sources that drive pneumatic actuators. A reversible reaction of water electrolysis was employed to generate gas pressure for pneumatic actuators (Suzumori, Wada, & Wakimoto, 2013), which was used as a power source for an untethered robot (Kitamori, Wada, Nabae, & Suzumori, 2016). Kitagawa et al. (2005) also proposed a portable pneumatic power source using the sublimation of dry ice to CO_2 gas. The devices above are limited in performance to the normal environment as against severe temperature environment. The mobility of the FFR in a high thermal environment, therefore, remains a concern.

The dry ice solid–gas phase transition has various application areas. Its sublimation to produce a large volume of CO_2 gas has been used to wipe out bed bugs in Nanoudon & Chanbang (2014). The effect of cloudy and non-cloudy air on the sublimation rate (SR) of dry ice was investigated by Kochtubajda & Lozowski (Kochtubajda & Lozowski, 1985). The study concluded that sublimation is faster in a warm, cloudy air and the result was used for cloud seeding. The sublimation of dry ice into gas in clear air was investigated in the experimental study of Winkel (2012). The production rate of CO_2 from dry ice was modeled, and the resulting model revealed that the SR of dry ice was proportional to its surface area. However, the majority of these applications have focused on producing a high volume of CO_2, while production time is not treated as a factor because of the application areas. For propulsion application where CO_2 will be used as a power source, both the volume and the sublimation time (ST) remain a design criterion.

To deliver sufficient power to drive the gas-driven motor, determination of the volume of CO_2 gas and mass of dry ice is critical. The following benchmark parameters, namely burning time for the fire scenario and volume of CO_2 gas are required to power the motor was computed in an earlier study (Ajala, Khan, Shafie, & Salami, 2017). From the study, we observed that the gas volume needed for a given time is a function of the mass of the dry ice and its SR. However, as dry ice SR is proportional to its surface area (Winkel, 2012), it becomes critical to determine the minimal size of dry ice that provides optimal SR at the shortest possible time. For instance, subliming the mass (say 30 g, for example) as a singular unit takes longer time than separate granules (say three 10 g sizes or two 15 g sizes). Hence, although the SR is critical to power the gas motor, the dry ice size also remains a design constraint. Also, increasing the rate of sublimation of dry ice is desirable at a relatively short burning time. According to Winkel (2012), dry ice sublimes faster in a warm environment than in cold ones. As a result, hot water is proposed as a means of speeding up the dry ice SR. Hence, with these underlying constraints, we selected dry ice mass and water temperature to optimally assess the sublimation of dry ice in a warm environment.

The air motor (Model No LG30FT, requires a gas supply of 4248 cm^3/s) (TONSON, 2015) to drive the FFR which will be powered using CO_2 gas *in situ* generated from dry ice. The motor is driven by the generated volumetric flow rate and pressure of the gas. As a result, three parameters need to be determined: time for production of gas, the volume of CO_2 gas, and generated gas pressure. As the expected operating environmental condition for the robot is at low pressure and moderate temperatures, the volume and pressure can be computed using the ideal gas equation and the equation of sublimation of dry ice to CO_2 gas. Since time cannot be calculated from these equations, the SR of dry ice will be used to predict the time required when sufficient volume and pressure of the CO_2 gas is produced to drive the robot. Due to limited data on SRs of dry ice in the literature (Chevrier, Roe, White, Bryson, & Blackburn, 2008), an experimental approach will be used to determine the SR of dry ice using hot water.

This paper presents the investigation of the production rate of CO_2 gas from the dry ice with the objective of using the gas to power a FFRin a high-temperature fire environment. Since the gas is expected to be self-generated from dry ice within the FFR with high response time, hot water is proposed as a catalyst to speed up the production rate. An experimental approach will be developed to optimize the SR of CO_2 gas for constraint applications such as the mass of dry ice and water temperature. The outcome would be an optimal water temperature and mass of dry ice that will be used for the prototype development of a CO_2 gas propulsion system. The gas propulsion system would be used to drive an autonomous FFR operating in a high thermal indoor fire environment. The rest of this report is organized as follows: Section 2 examines the materials, methods as well as the design of experiments (DOEs). The results and analysis are discussed in Section 3, while the optimization analysis is presented in Section 4. The summary and conclusion are given in Section 5.

2. Materials and methods

2.1. Materials

The sample masses of dry ice for the experiment were in the range of 15–35 g (step increase of 5 g). Each sample used in this study was taken from the 5000-g blocks purchased from Linde Gas (The Linde Group,

2009). Hot water at 60°C, 70°C, and 80°C was used for the experiment based on the realization reported in Ajala et al. (Ajala et al., 2016) that the SR below 60°C is negligibly small. Type-K Glass Braid Insulated–K thermocouple (with MAX31,855 breakout board amplifier) was used to measure the water temperature. Both the thermocouple and its amplifier were used with Arduino Uno board (UNO R3; based on the ATmega328 microcontroller) for data logging.

2.2. Experimental design

Statistical DOE is a method of designing a series of tests where the control variables (also known as control factors) are modified by a specified order to identify the reasons for the changes in the response parameters (Cavazzuti, 2012). There are various DOE techniques for experimental design, which include full-factorial design (FFD), response surface methodology (RSM), and Taguchi orthogonal array (TOA) method, among others. However, the choice of methods depends mainly on the aim of the experimentation (Cavazzuti, 2012). DOE is widely employed in many industrial and academic types of research for product and process design and/or optimization.

From our literature search, no studies have used dry ice to power a pneumatic motor, as well as use hot water to speed up the rate of sublimation of dry ice for the same purpose. So, this study employs a DOE technique using FFD and RSM approaches for design and optimizing CO_2 production rates for a FFR pneumatic actuation application. Figure 1 illustrates the process flowchart for the RSM statistical DOE employed in this study. The experimental approach is divided into three stages —planning stage, an execution stage, and analysis and optimization stage.

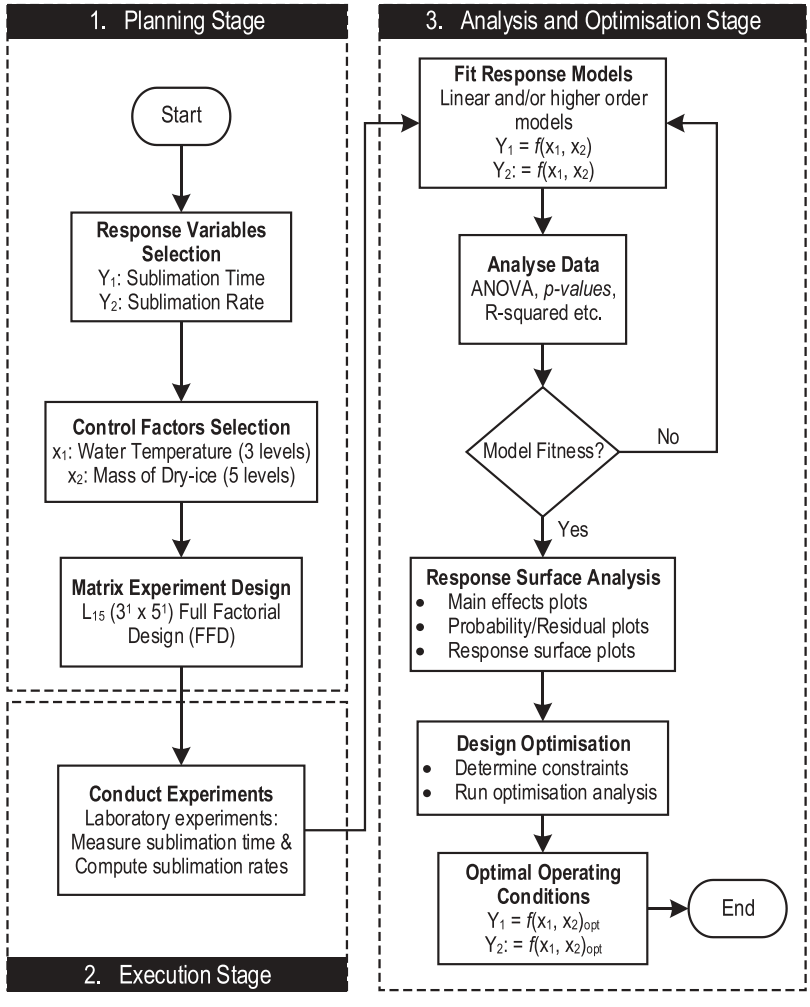

Figure 1. Flowchart of the response surface method for experimental design and optimization.

Table 1. Experimental control factors and their levels

Factors	Units	Levels				
		1	2	3	4	5
Water temperature	°C	60	70	80		
Dry ice mass	g	15	20	25	30	35

2.2.1. Experimental planning

The planning stage consists of (a) the selection of the response variables as ST (Y_1) and SRs (Y_2); (b) the selection of the control factors as water temperature (X_1) and mass of dry ice (X_2). Three levels were selected for the water temperature and five levels for the mass of dry ice (see Table 1) to cover the experimental region. Upon the selection of response and design variables, the next step is the matrix experiment design.

With the levels of the control factors, we employed a $3^1 \times 5^1$ full-factorial design, thereby leading to a 15 run experimental (i.e., L_{15}) matrix (Table 2). Full-factorial design provides detailed information about the experimental design space. Hence, it is adjudged as a better choice in statistical experimental design (Barker & Milivojevich, 2016). However, full-factorial design becomes an expensive choice as the number of design factors increases. Nonetheless, with only two design factors involved in this study, the full-factorial design is considered adequate.

2.2.2. Experimental setup and data collection

Upon the selection of responses, control factors, and experimental matrix design, the next stage in the statistical design of the experiment is data collection. Figure 2 shows the schematic of the experimental setup for the study. Its main components were divided into the measurement, data acquisition, and data logging. The measurement system consists of a container and Type-K Glass Braid Insulated–K thermocouple that is immersed in water to measure the water temperature. The data acquisition consists of an Arduino Uno R3 microcontroller and MAX 31,855 amplifier that interface between the thermocouple and the microcontroller. The data logging consist of a personal computer with Tera term software that communicates with the microcontroller and simultaneous data displaying and logging. A series of jumpers and cables connected the setup.

Table 2. L_{15} (3^1 x 5^1) FFD experimental design matrix

Run	X_1 (°C)	X_2 (g)
1	70	35
2	60	35
3	60	15
4	80	25
5	70	15
6	70	25
7	80	35
8	70	20
9	70	30
10	80	30
11	60	25
12	60	30
13	80	20
14	60	20
15	80	15

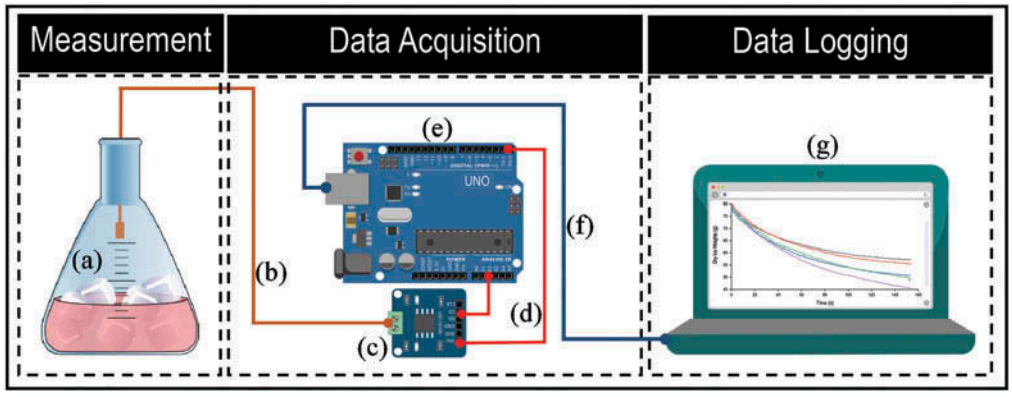

Figure 2. Dry ice–hot water experimental setup (a—Dry ice and hot water container; b—K-type thermocouple; c—MAX 31855 Amplifier; d—Jumpers for connections; e—Arduino Uno R3 Microcontroller; f—USB connection cable g-Laptop).

The container used for measurement is a transparent 1750 cm^3 jar. For each of the experimental trial shown in Table 2, the container is filled with 200 cm^3 of water, which was allowed to cool down to the desired temperature. After that, the desired sample mass of the dry ice is cut from a 5000-g slab dry ice, weighed, and recorded. The temperature of the cooling water was monitored with the thermocouple with the data displayed and logged on the personal computer. The moment the desired temperature is achieved the Arduino controller is reset with the aid of an onboard reset switch and the sample mass of dry ice is dropped into the 200 cm^3 water in the open container.

Furthermore, the temperature of water at the beginning and end of the sublimation of the dry ice were recorded. The sublimation of dry ice in hot water is then observed and the time (Y_1) for the sample mass to completely sublime is logged with the test equipment described earlier. This process is repeated for the experimental matrix presented in Table 2.

2.2.3. Experimental data analysis

For each of the ST (Y_1) obtained during each of the experimental trials, the SR (Y_2) was computed using Equation (1) as documented in the study of Murphy and McSweeny (2013). The sublimation rate is denoted by *SR*, mass by *m,* and time by *t* in the equation. The experiments were conducted in a random order to limit the errors due to instrumentation and data collection procedures. Additionally, to further prevent inherent measurement errors the experimental runs were performed in triplicates, and the average presented.

$$SR = f(m, t) \tag{1}$$

Response surface methodology (RSM) was used for the data analysis to examine the effect of water temperature and dry ice mass on the sublimation rates of dry ice. This is because RSM is suitable for continuous control factor (e.g., time, mass) and also when the objective is to optimize the response variable(s) of interest (Khoei, Masters, & Gethin, 2002). In the RSM approach, using the selected experimental data, a polynomial function was used to fit models that describe the relationship between the control factors and response variables. Equation (2) (Montgomery, 2001) shows the polynomial function that describes the relationship between the control factors and response variables.

$$Y = a_0 + \sum_{i=1}^{k} a_i X_i + \left(\sum_{i=1}^{k} a_{ii} X_i\right)^2 + \sum_{i=1}^{k-1} \sum_{j=i+1}^{k} a_{ij} X_i X_j + \varepsilon \tag{2}$$

where *Y* represents the response, a_0 is the intercept; a_i is the coefficient of linear factor effects, a_{ij} is the interaction coefficient, a_{ii} is the quadratic coefficients, and ε is the error terms. Upon the completion of data fitting, the next step in the data analysis is showing the main effects of the control factors. This is subsequently followed by the evaluation of the analysis of variance (ANOVA)

to validate the significance of the models and assess the relative importance of the control factors. ANOVA analysis involves the estimation of the sum of squares values from different factors. The experimental design and statistical analysis were conducted using Design-Expert® software (Stat Ease Inc., 2015). The model-fitting was tested regarding the coefficient of determination (i.e., R^2, Adjusted R^2, and Predicted R^2.) and the level of probability, i.e., *p*-values.

The validity of the RSM-fitted model to the experimental dataset is based on three assumptions: (a) that the treatment population be normally distributed, (b) the variance of the observation is each treatment be equal, and (c) the observation be randomly selected from the treatment population (Pan, 2016), (Khan, 2013). Thus, it is essential to conduct quality assurance checks on the experimental dataset to ensure the suitability of the RSM-fitted model to the data. The quality assurance consists of normality, constant variance, and independence tests, which are, respectively, conducted with normal probability plot of residuals, Residuals versus Fit plot, and Residual versus order plot. As such, this study developed and assessed the residual plots to ascertain the RSM application validity assumptions.

Having fitted the model and ascertain their validity, it is of interest in this study to know the best settings for the control factors. Hence, we carried out an optimization study to assess the control factors' (i.e., water temperature, and mass of dry ice) settings that optimize the ST and SRs.

3. Results and discussion

3.1. Response analysis

Table 3 presents the experimental results for the two response variables, i.e., ST and SRs under different control factors' (i.e., water temperature and mass of dry ice) settings. The response for the SR is in the range of 0.0718–0.1563 g/s, while that of the ST falls between 153.5–209 s. The experimental data were analyzed in order to measure temperature and mass effect on the sublimation of dry ice.

3.1.1. Model-fitting

Regression computations fitting all the polynomial models to the responses were performed to generate an acceptable model. The sequential model sum of squares and model summary statistic tests were applied for this purpose. The tests calculate the effects of all the model

Table 3. Experimental design with the responses

Run	X_1 (°C)	X_2 (g)	ST (s)	SR (g/s)
1	70	35	283	0.1237
2	60	35	298.5	0.1173
3	60	15	209	0.0718
4	80	25	200	0.1250
5	70	15	176	0.0852
6	70	25	209	0.1196
7	80	35	224	0.1563
8	70	20	213.5	0.0937
9	70	30	251	0.1195
10	80	30	209	0.1435
11	60	25	257	0.0973
12	60	30	275.5	0.1089
13	80	20	190.5	0.1050
14	60	20	261	0.0766
15	80	15	153.5	0.0977

terms and the results are displayed in Tables (4,5). From Table 4, a linear model is found as the most appropriate. This is because the linear model produces high *F* values of 103.22 for SR and 76.44 for ST; with corresponding low *p*-values (<0.0001).

Model summary statistics' result presented in Table 5 confirms the suitability of the linear model. This is because the model exhibits a low standard deviation (0.00594 and 12.18 for SR and ST, respectively), high R^2 values (0.9451 for SR and 0.9272 for ST), and a corresponding least value of predicted residual sums of squares (0.00064 for SR and 2735.32 for ST) for both the SR and ST. A reasonable agreement between the difference in the values of the Adjusted R^2 and Predicted R^2 (0.0186 for SR and 0.0269 for ST) is also observed from Table 5. This also validates the acceptance of the linear model because the reasonable difference should be lower than 0.2 (Montgomery, 2001).

R^2 indicates the amount of relationship of the response variable to the combined linear predictor variables. Therefore, the R^2 value of 0.9451 and 0.9271 (Table 5) implies that the model can explain more than 94% of the experimental data for the SR and 92% for the ST. The high value of the adjusted R^2 and Predicted R^2 is also an indication of a strong relationship between the observed and the predicted values.

3.1.2. Model adequacies

Following the satisfactory fitting result displayed from the model diagnosis above, a quality assurance test to check the normality of the data. This is displayed as a normal probability plot of residuals for the response variables in Figure 3. The distribution of the data around the half-normal plots (i.e., the straight line) in Figure 3(a,b) indicates that the residuals follow a normal distribution. Also, the scattering of the data randomly between the red lines in Figure 4(a,b) further confirms the assumption of constant variance and the absence of outliers. In other words, as the assumption of normality is satisfied, the model generally fits all the data well.

3.1.3. Mathematical model development

The mathematical relationship between the responses and the control factors in terms of the coded and actual values of the variables is presented in Equations (3)–(6). The coded equations

Table 4. Sequential model sum of squares

Source	Sum of squares	df	Mean square	*F* value	*p-value* Prob > *F*	Remark
(a) Sublimation rate (SR)						
Mean vs Total	0.18	1	0.18			
Linear vs Mean	7.28×10^{-3}	2	3.64 x 10–3	103.22	≤0.0001	Suggested
2FI vs Linear	5.249×10^{-5}	1	5.249×10^{-5}	1.56	0.2379	
Quadratic vs 2FI	2.589×10^{-5}	2	1.295×10^{-5}	0.34	0.7219	
Cubic vs Quadratic	1.798×10^{-4}	3	$5.993x\ 10^{-5}$	2.18	0.1915	Aliased
Residual	1.65×10^{-4}	6	2.751×10^{-5}			
Total	0.19	15	0.012			
(b) Sublimation time (ST)						
Mean vs Total	775,400	1	775,400			
Linear vs Mean	22,678.27	2	11,339.14	76.45	≤0.0001	Suggested
2FI vs Linear	57.8	1	57.8	0.37	0.5558	
Quadratic vs 2FI	52.78	2	26.39	0.14	0.8693	
Cubic vs Quadratic	907.09	3	302.36	2.38	0.1685	Aliased
Residual	762.28	6	127.05			
Total	799,900	15	53,326.15			

Table 5. Model summary statistics

Source	Std. Dev.	R^2	Adjusted R^2	Predicted R^2	PRESS	Remark
(a) Sublimation rate						
Linear	5.939×10^{-3}	0.9451	0.9359	0.9173	6.371×10^{-4}	Suggested
2FI	5.805×10^{-3}	0.9519	0.9388	0.9251	5.773×10^{-4}	
Quadratic	6.19×10^{-3}	0.9552	0.9304	0.8825	9.053×10^{-4}	
Cubic	5.245×10^{-3}	0.9786	0.95	0.7905	1.614×10^{-4}	
(b) Sublimation time						
Linear	12.18	0.9272	0.9151	0.8882	2735.32	Suggested
2FI	12.51	0.9296	0.9104	0.874	3082.65	
Quadratic	13.62	0.9317	0.8938	0.8253	4273.25	
Cubic	11.27	0.9688	0.9273	0.6849	7706.69	Aliased

given in Equations (3) and (4) are useful for identifying the relative impact of the factors by comparing the factor coefficients. Thus, it can be deduced from Equations (3) and (4) that the mass of dry ice (coefficients of 0.0255 and 40.30) has a more significant effect on sublimation of dry ice than water temperature (coefficients of 0.016 and −32.40).

$$Y_1 = +0.11 + 0.016X_1 + 0.0255X_2 \tag{3}$$

$$Y_2 = +227.37 - 32.40X_1 + 40.30X_2 \tag{4}$$

where: Y_1= Sublimation rate (g/s); Y_2= Sublimation time (s); X_1 = water temperature (°C), and X_2 = dry ice mass (g).

The equation in terms of the actual values of the factors is shown in Equations (5) and (6). These equations are useful to predict the response for given levels of each of the control factors. These models are valid within the region of the experimental design, that is, the applied range of the experimental control parameters of this research.

$$Y_1 = -0.063147 + 0.001556X_1 + 0.002545X_2 \tag{5}$$

$$Y_2 = 353.41667 - 3.24X_1 + 4.03X_2 \tag{6}$$

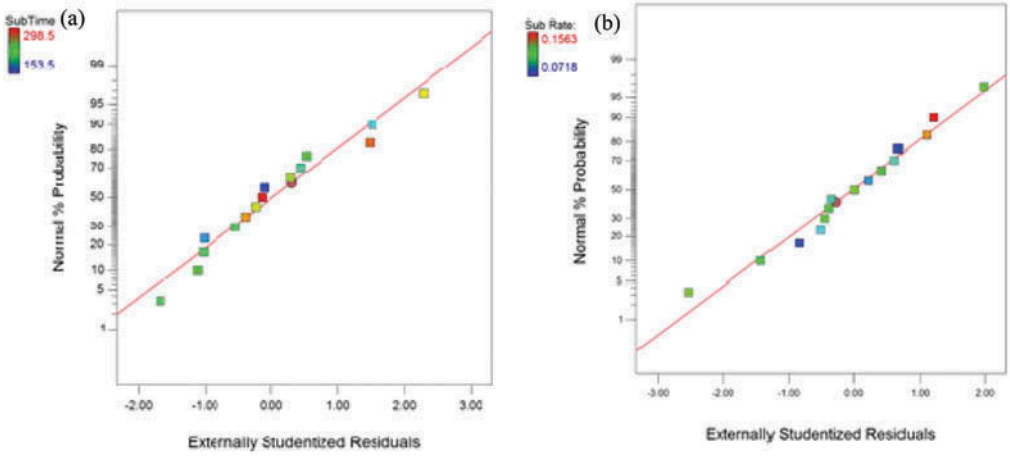

Figure 3. Normal plot of residuals for sublimation (a) Time response and (b) Rate response.

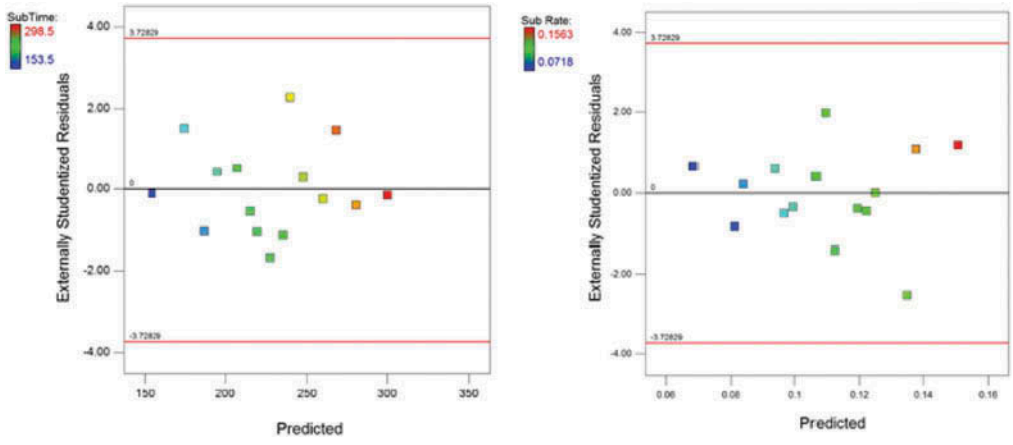

Figure 4. Residual vs Predicted for (a) Sublimation Time and (b) Sublimation rate.

3.1.4. Analysis of variance (ANOVA) of the fitted model

The statistical significance of the linear model was estimated using the ANOVA technique, and the results are presented in Table 6. The ANOVA proved that the selected linear model is suitable (i.e., significant). This is due to the high *F*value with a corresponding low *p*-value (<0.0001). Hence, the two factors Water Temperature (X_1) and Dry ice Mass (X_2) in Table 5 are regarded as significant model terms at a 95% confidence level.

3.2. Effects of control factors on the response variables

3.2.1. Contour and 3D surface plots

A 2D graphical representation of the relationship between the responses and the control factors is presented as contour plots in Figure 5(a,b) in order to visualize the control factors' effects. The plots demonstrate that both factors have an individual effect (i.e., the main effect) on both the ST and the SR. Thus, variation in the factors results in changes in the responses. The ST increased at higher masses of dry ice (Figure 5(a)), while Figure 5(b) revealed that a high SR is achieved by subliming large masses of dry ice at higher water temperature.

The linear variation effect becomes more visible with a three-dimensional (3D) surface plots shown in Figure 6(a,b). These plots indicated that there is no interaction effect of the mass of dry ice and the water temperature on both the ST and the SR. Figure 6(a) shows the effect of water temperature and dry ice mass on the ST. The results revealed that the ST is increasing as large masses of dry ice sublimes. It, however, decreases when the temperature increases. An increased SR is achieved at both higher dry ice masses and water temperature as indicated in Figure 6(b)

3.2.2. Main effect plots

The goal of this experiment is to study the influence water temperature on the different masses of dry ice such that volume requirement of CO_2 gas can be produced to satisfy the 4250 cm^3/s consumption rate of the selected pneumatic motor. Given this, a short time response for the gas production is desirable. To achieve this, the main effect plot using the data means was employed to study the influence of each of the factors (water temperature and mass of dry ice) on the SR and ST of dry ice. This is presented in Figures 7 and 8, respectively.

Figures 7 and 8 show the main effects of the control factors on the ST and SRs. Figure 7 provides the effects of water temperature on both the SR (Figure 7(a)) and ST (Figure 7(b)) of dry ice. The linearly increasing relationship shown in Figure 7(a) suggests that the water temperature aid the SRs, with the highest SR of 0.1563 g/s recorded at the highest

Table 6. ANOVA for the response surface of the linear model

Source	Sum of Squares	df	Mean Square	*F* value	*p*-value Prob > *F*	Remark
(a) Sublimation rate						
Model	7.28×10^{-3}	2	3.64×10^{-3}	103.22	<0.0001	Significant
X_1	2.421×10^{-3}	1	2.421×10^{-3}	68.65	<0.0001	
X_2	4.859×10^{-3}	1	4.859×10^{-3}	137.78	<0.0001	
Residual	4.232×10^{-4}	12	3.527×10^{-5}			
Cor total	7.703×10^{-3}	14				
(b) Sublimation time						
Model	22,678.27	2	11,339.14	76.45	<0.0001	Significant
X_1	10,497.6	1	10,497.6	70.77	<0.0001	
X_2	12,180.68	1	12,180.68	82.12	<0.0001	
Residual	1779.96	12	148.33			
Cor total	24,458.23	14				

temperature (80°C). The result is consistent with findings of Winkel (2012) and Kochtubajda & Lozowski (1985) that sublimation is faster in a warm environment. Also for every 10°C rise in temperature, about 0.016 g of dry ice sublimes in 1 s. Figure 7(b), however, indicates that ST decreases for every increase in temperature. The highest temperature (80°C) resulted in a minimum ST of 153.5 s. Similar to SRs, the ST is reduced by 32.4 s for every 10°C rise in temperature. These two conditions are desirable for the present study.

The mass effect plot in Figure 8(a) also produces a high SR as the dry ice mass increases. This is consistent with the findings that high mass of dry ice produces a high concentration of CO_2 gas (i.e., the high volume of the gas). Conversely, the high volume (produced at 80°C,

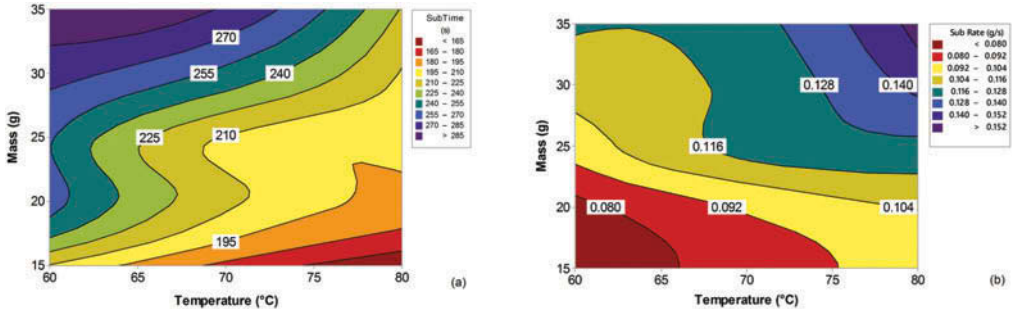

Figure 5. 2D plot (a) sublimation time and (b) sublimation rate.

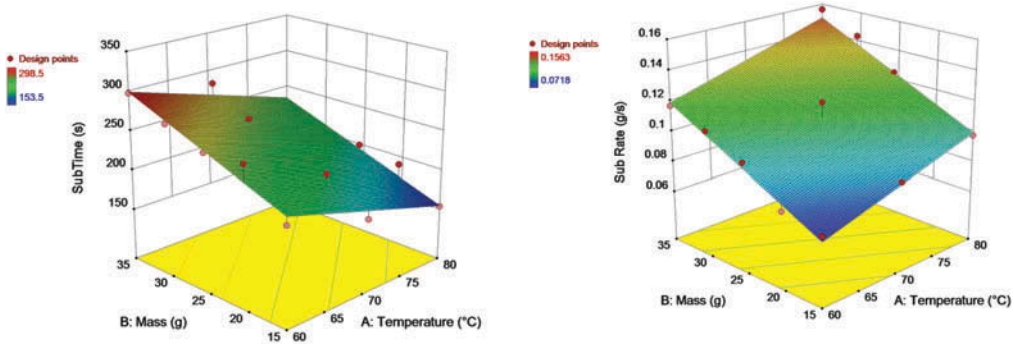

Figure 6. 3D surface plot (a) sublimation time and (b) sublimation rate.

35 g, 0.5678 g/s) comes with a time constraint. At this factors' combination, the long ST of 224 s as indicated in Figure 8(b) will lead to delay in the actuation of the FFR, which is undesirable. The deduction from Figure 8(a) has been the strength of the majority of the earlier studies cited on the SRs of dry ice to generate CO_2 gas in the introduction section. They focus on creating a large volume of the gas from dry ice giving preference to the volume of the gas only. As such, short time of sublimation for the gas production along with the method of achieving the short time response becomes less critical due to their application areas.

A consideration for the size of the dry ice can also be a useful design criterion in addition to the use of hot water to achieve the short time of sublimation because the dry ice SR is proportional to its size (Winkel, 2012). Also optimizing the SR alone without proper consideration for dry ice mass will delay the achievement of the required gas volume in FFR consideration. In the FFR application, the two parameters (water temperature and dry ice mass) as well the SR are essential. This is because high response time (i.e., short time of sublimation) is required for the dry ice sublimation of the CAFFR suggested in our earlier study (Ajala et al., 2016). Implementing this will make the CAFFR to operate successfully inside an indoor fire when the fire has already started. Results from Figures 7 and 8 when taken together suggest the need to optimize the SR and other parameters.

4. Parametric optimization

The aim of this study is to determine the maximum water temperature that will accelerate sublimation of a given mass of dry ice in minimal time and produce an optimum SR in order to achieve the flow requirement of the air motor. Thus, the optimization component in Design-Expert ® 9 (Stat Ease Inc., 2015) was adopted.

4.1. Optimization criteria with solution

The SR is maximized and set to the highest level of importance. Also, the water temperature is maximized, whereas both the ST and mass of dry ice are minimized thereby set to the same

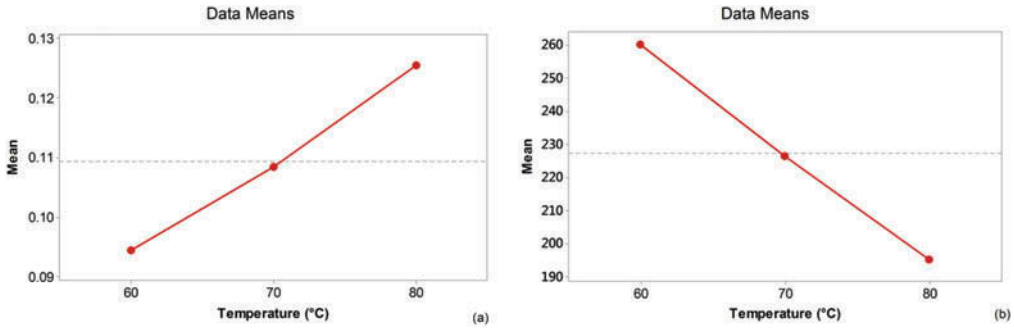

Figure 7. Main effects plot of temperature for (a) sublimation rate and (b) sublimation time.

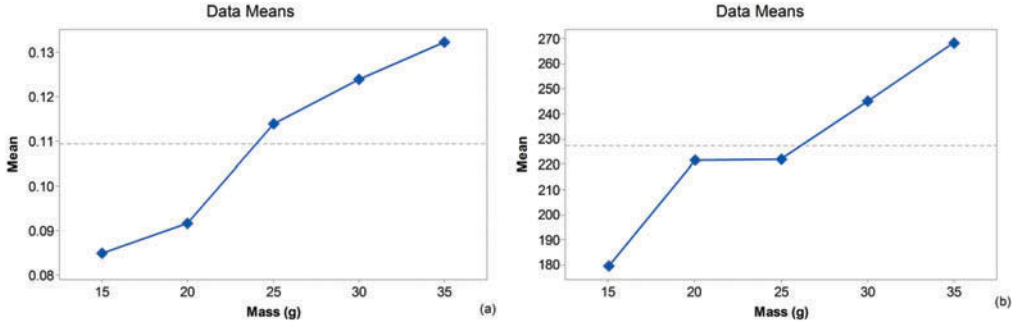

Figure 8. Main effect plots of mass of dry ice for (a) sublimation rate and (b) sublimation time.

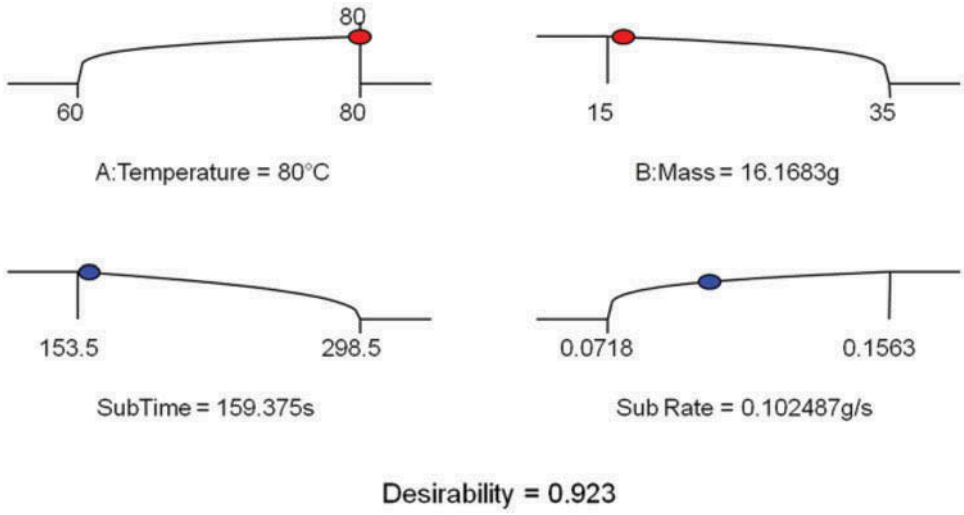

Figure 9. Optimization ramp graph.

level of importance. Solutions are then found using numerical optimization node. The result obtained from the optimization is displayed in Figure 9. The solution that came out as the optimum for the SR, water temperature, mass of dry ice, and ST is 0.1025 g/s, 80°C, 16.1683 g, and 159.375 s, respectively, with a desirability 0.923. The 3D plot of the desirability of the optimization is given in Figure 10. Also, the 3D plot for the optimal SR and ST are displayed in Figures 11 and 12, respectively.

5. Conclusion

This study examined the effect of water temperature on the SRs of different masses of dry ice. During this investigation, the DOEs based on response surface methodology was utilized to optimize the SR and ST based on water temperature and mass of dry ice. This is done in

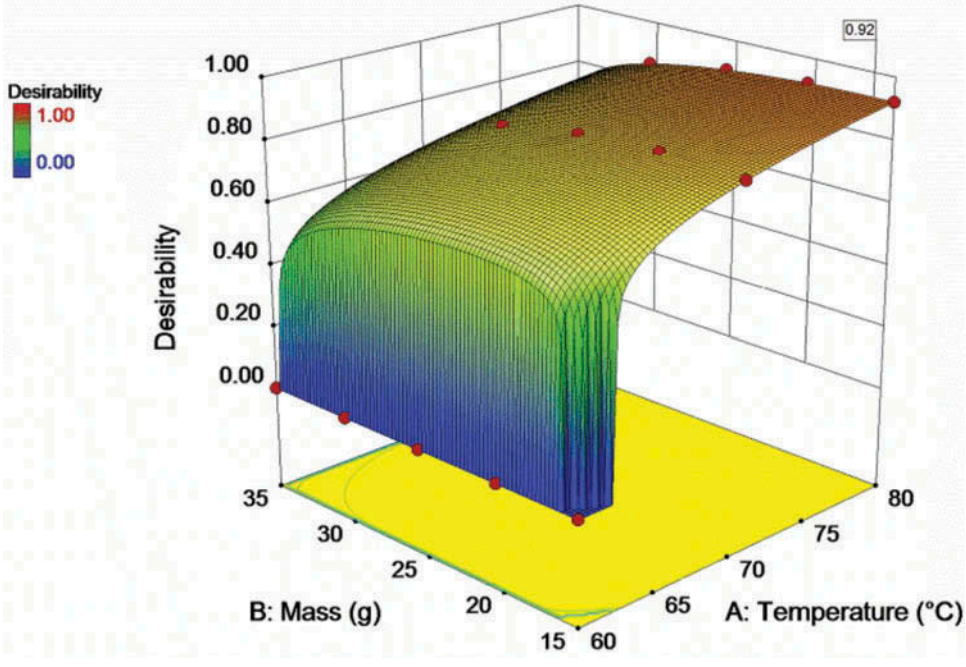

Figure 10. Desirability 3D surface plot.

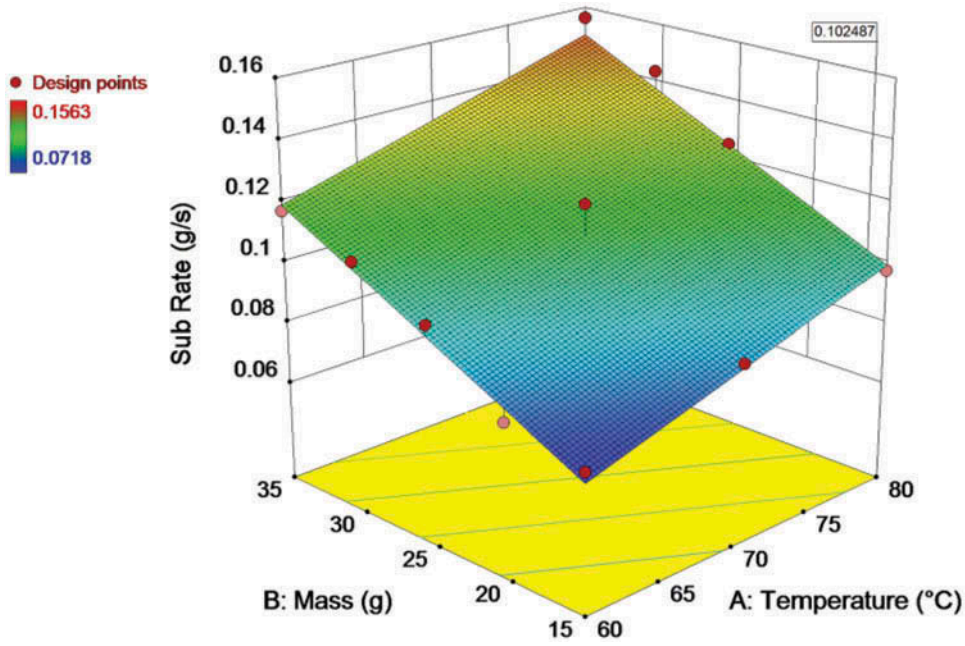

Figure 11. 3D surface plot optimal sublimation rate.

order to predict the production rate of CO_2 from dry ice along with the pressure requirement of a pneumatic motor for pneumatic power generation. Hot water at 60°C, 70°C, and 80°C were used to accelerate the sublimation of dry ice. The obtained results have indicated that higher water temperature will increase the SR and decrease ST which is necessary for the quick response of the actuator. Also, increasing the dry ice mass will increase ST. Hence, the best approach is to minimize ST in order to generate quick pressure response. An optimal SR

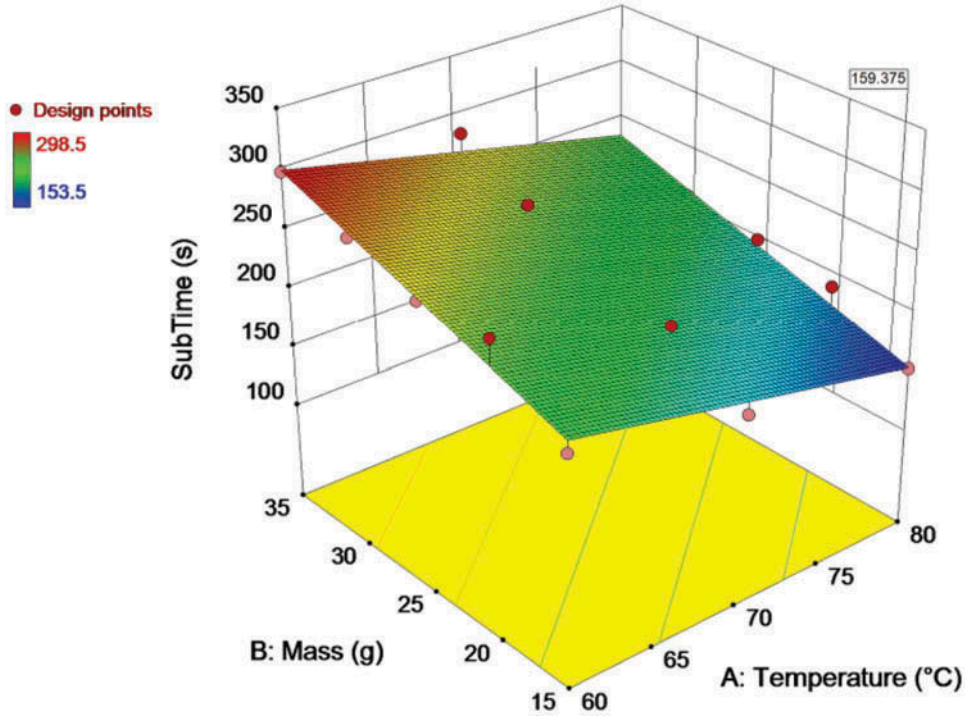

Figure 12. 3D surface plot of the optimal sublimation time.

value of 0.1025 g/s is obtained at a temperature of 80°C, mass of 16.1683 g, and ST of 159.375 s. Results obtained in this investigation provide a solid foundation for the optimization of CO_2 SR in the generation of the gas pressure required to power a pneumatic motor. It will also be used as the basis for the completion of the prototype development. Although the pneumatic motor, in this study, will be used to propel a FFR in the high thermal indoor fire, the same approach is applicable in other highly constrained applications. The approach is scalable as more factors (e.g., container insulation that is assumed to be constant in the current study) can be included for further optimization.

Funding
The authors received no direct funding for this research.

Author details
M. T. Ajala[1,2]
E-mail: mosud.ajala@yahoo.com
ORCID ID: http://orcid.org/0000-0002-3461-601X
Md R. Khan[1]
E-mail: raisuddin@iium.edu.my
A. A. Shafie[1]
E-mail: aashafie@iium.edu.my
M. J. E. Salami[3]
E-mail: mjesalami@gmail.com
M. I. Mohamad Nor[4]
E-mail: misk@um.edu.my
M. O. Oladokun[5]
E-mail: lyday011@gmail.com
[1] Department of Mechatronics Engineering, International Islamic University Malaysia, Gombak, Kuala Lumpur.
[2] Department of Industrial Maintenance Engineering, Yaba College of Technology, Yaba, Lagos State, Nigeria.
[3] Aliko Dangote Foundation, Victoria Island, Lagos State, Nigeria.
[4] Department of Chemical Engineering, University of Malaya (UM), Kuala Lumpur, Malaysia.
[5] Department of Architectural and Civil Engineering, City University of Hong Kong, Kowloon Tong, Hong Kong, China.

Cover Image
source:

Citation information
Cite this article as: Optimization of CO_2 production rate for firefighting robot applications using response surface methodology, M. T. Ajala, Md R. Khan, A. A. Shafie, M. J. E. Salami, M. I. Mohamad Nor & M. O. Oladokun, *Cogent Engineering* (2018), 5: 1555744.

References

Ajala, M. T., Khan, M. R., Shafie, A. A., & Salami, M. J. E. (2017). Prediction of dry ice mass for firefighting robot actuation. *In IOP Conference Series: Materials Science and Engineering, 260*(1), 012023.

Ajala, M. T., Khan, M. R., Shafie, A. A., & Salami, M. J. E. (2016). Development of a New Concept for Fire Fighting Robot Propulsion System. In *International Conference on Material, Industrial and Mechanical Engineering (ICMIME2016)* (pp. 90–91). Kuala Lumpur, Malaysia: ICONTES2016.

AlHaza, T., Alsadoon, A., Alhusinan, Z., Jarwali, M., & Alsaif, K. (2015). New concept for indoor fire fighting robot. *Procedia – Social and Behavioral Sciences*, *195*, 2343–2352. doi:10.1016/j.sbspro.2015.06.191

Amano, H. (2002). Present status and problems of fire fighting robots. In *SICE 2002. Proceedings of the 41st SICE Annual Conference* (Vol. 2, pp. 880–885). Osaka: IEEE. doi:10.1109/SICE.2002.1195276

Barker, T. B., & Milivojevich, A. (2016). *Quality by experimental design* (4th ed.). Boca Raton: CRC Press.

Cavazzuti, M. (2012). *Optimization methods: From theory to design scientific and technological aspects in mechanics* (1st ed.). Berlin, Heidelberg: Springer-Verlag.

Chevrier, V. F., Roe, L. A., White, K. F., Bryson, K., & Blackburn, D. G. (2008). Sublimation kinetics of CO2 ice on the surface of mars. In *Lunar and Planetary Science Conference* (pp. 1178). League City, Texas.

Haynes, H. J. G., & Molis, J. L. (2016). *U.S. Firefighter injuries –2015*. Quincy: NFPA.

Khan, R. M. (2013). Design of experiment. *Problem solving and data analysis using minitab*. West Sussex: John Wiley & Sons, Ltd.

Khoei, A. R., Masters, I., & Gethin, D. T. (2002). Design optimisation of aluminium recycling processes using taguchi technique. *Journal of Materials Processing Technology*, *127*(1), 96–106. doi:10.1016/S0924-0136(02)00273-X

Kitamori, T., Wada, A., Nabae, H., & Suzumori, K. (2016) Untethered three-arm pneumatic robot using hose-free pneumatic actuator. In *2016 IEEE/RSJ International Conference on Intelligent Robots and Systems (IROS)* (pp. 543–548). Daejeon, Korea: IEEE. doi:10.1109/IROS.2016.7759106.

Kochtubajda, B., & Lozowski, E. P. (1985). The sublimation of dry ice pellets used for cloud seeding. *Journal of Climate And. Applied Meteorology*, *24*(6), 597–605. doi:10.1175/1520-0450(1985)024<0597:TSODIP>2.0.CO;2

Liljebäck, P., Stavdahl, Ø., & Beitnes, A. (2006). SnakeFighter – Development of a water hydraulic fire fighting snake robot. In *Control, Automation, Robotics and Vision, 2006. ICARCV '06. 9th International Conference on* (pp. 1–6). Singapore: IEEE.

Matsuoka, H., & Suzumori, K. (2014). Gas/liquid phase change actuator for use in extreme temperature environments. *International Journal of Automotive Technology*, *8*(2), 140–146. doi:10.20965/ijat.2014.p0140

Matsuoka, H., Suzumori, K., & Kanda, T. (2016). Development of a gas/liquid phase change actuator for high temperatures. *Robotics and Mechatronics*, *3*(1), 1–7. doi:10.1186/s40648-016-0041-7

Montgomery, D. C. (2001). *Design and analysis of experiments* (5th ed.). New York, NY: John Wiley & Sons Inc. Retrived from https://doi.org/10.1002/qre.4680030319

Murphy, J. M., & McSweeny, T. I. (2013). *Technical assessment of dry ice limits on aircraft*. Washington.

Nanoudon, S., & Chanbang, Y. (2014) Use of solid carbon dioxide for controlling bed bugs cimex hemipterus (fabricius) under laboratory conditions. In *JITMM 2013 Proceedings* (pp. 55–61). Bangkok.

Ono, M., & Kato, S. (2010). A study of an earthworm type inspection robot movable in long pipes. *International Journal of Advanced Robotic Systems*, *7*(1), 85–90. doi:10.5772/7248

Pan, J. J. 2016. Minitab tutorials for design and analysis of experiments online. [Online]. Retrieved Jul 24, 2016. from https://www.wpi.edu/Pubs/ETD/Available/etd-082714-135653/unrestricted/How_to_Use_Minitab_4_Design_of_Experiments.pdf

Stat Ease Inc. (2015). *Design-expert software version 9.0.6.2*. Minneapolis, MN: USA.

Suzumori, K., Matsuoka, H., & Wakimoto, S. (2012). Novel actuator driven with phase transition of working fluid for uses in wide temperature range. In *Intelligent* Robots *and* Systems (IROS), *2012 IEEE/RSJ International Conference on* (pp. 616–621). Algarve, Portugal: IEEE.

Suzumori, K., Wada, A., & Wakimoto, S. (2013). A new mobile pressure control system for pneumatic actuators, using reversible chemical reactions of water. In *IEEE/ASME International Conference on Advanced Intelligent Mechatronics (AIM)* (pp. 122–127). Wollongong, Australia: IEEE. doi:10.1016/j.sna.2013.07.008

The Linde Group. (2009). Safety data sheet carbon dioxide, solid (dry ice). *Creation date*. [Online]. Retrieved April 18, 2016 from http://www.linde-gas.com/internet.global.lindegas.global/en/images/Solid carbondioxide17_24380.pdf

Tonson. (2015). *M3-LG30: Tonson air motors mfg corp.* Taiwan. RetrievedDecember 18, 2015, from http://www.tonson-motor.com/e/p001.htm

Winkel, B. (2012). Modelling sublimation of carbon dioxide. *International Journal of Mathematical Education in Science and Technology*, *43*(8), 1077–1085. doi:10.1080/0020739X.2011.644336

Wu, H., Kitagawa, A., & Tsukagoshi, H. (2005). Development of a portable pneumatic source using phase transition at the triple point (pp. 310–315). Tsukuba: JFPS.

Zhang, L., Kitagawa, A., & Tsukagoshi, H. (1999). A study on water hydraulic fire-fighting robot. *Proceedings JFPS International Symposium on Fluid Power, 1999* (4), 727–732. doi:10.5739/isfp.1999.727

Cogent Engineering **(ISSN: 2331-1916) is published by Cogent OA, part of Taylor & Francis Group.**

Publishing with Cogent OA ensures:

- Immediate, universal access to your article on publication
- High visibility and discoverability via the Cogent OA website as well as Taylor & Francis Online
- Download and citation statistics for your article
- Rapid online publication
- Input from, and dialog with, expert editors and editorial boards
- Retention of full copyright of your article
- Guaranteed legacy preservation of your article
- Discounts and waivers for authors in developing regions

Submit your manuscript to a Cogent OA journal at www.CogentOA.com